C.P. No. 966

C.P. No. 966

MINISTRY OF TECHNOLOGY

AERONAUTICAL RESEARCH COUNCIL

CURRENT PAPERS

Some Further Notes on the Laminar Boundary Layer Development and Running Time in a Shock Tube

By

J. A. D. Ackroyd

LONDON: HER MAJESTY'S STATIONERY OFFICE
1967

Price 8s 6d. net

C.P. No. 966*

Some Further Notes on the Laminar Boundary Layer Development and Running Time in a Shock Tube

by

J. A. D. Ackroyd

---

*Replaces A.R.C.26 457

SUMMARY

Bernstein's analysis of the laminar boundary layer development aft of a shock wave in a shock tube is corrected in the light of more recent theoretical results. The analysis is extended to include certain pressure gradient corrections. Ackroyd's analysis of the running time in a shock tube, which was based on Bernstein's work, is also re-examined. The corrected results show a significant change in boundary layer characteristics and running time as compared with Bernstein's results. However, the effects of the additional pressure gradient corrections are shown to be negligible.

CONTENTS

I Introduction.

Bernstein, in his analysis presented in ref.1, examines the unsteady growth of the laminar boundary layer induced by the passage of the primary shock wave along the channel of a shock tube. He has assumed that there is no attenuation of the shock wave and is able, therefore, to reduce the equations of motion to a quasi-steady form by considering the flow relative to the shock wave. The analysis is based on the channel flow integral momentum and mass flow equations and the solution of these equations requires knowledge of the nature of the wall friction in the channel and the form parameter (which is the ratio of the displacement and momentum thicknesses for the channel flow boundary layer). Thus, in order to solve these equations, Bernstein makes two important assumptions. The first is that expressions for the channel flow wall friction and form parameter may be taken to be the same as those on a moving plate which experiences the same external flow conditions as those existing in the inviscid core of the channel flow. The second assumption is that relative to the wall the velocity profile for the shock-induced boundary layer is similar to the velocity profile for a steady laminar compressible boundary layer. The first assumption is valid provided that the boundary layer in the channel does not become so thick as to be comparable to the radius of the channel.

This assumption is retained in the present paper. In ref.3, it is shown that the velocity profile for a laminar shock-induced boundary layer depends principally on the ratio of the wall velocity to that of the inviscid flow (the flow being viewed relative to the moving shock wave). Clearly, the second of Bernstein's assmuptions is unjustified and work presented in refs. 2 and 4 is used to correct Bernstein's work here.

Although the effects of pressure gradients are accounted for in the major part of the work outlined above, it is necessary to assume that pressure gradients are zero in developing expressions for two important parameters. These parameters are both based on velocities measured relative to the wall, in which case a strong similarity is noted in the behaviour of these parameters when compared with the behaviour of the corresponding parameters for the steady boundary layer. The parameters are the form parameter, H, and a shape parameter, f, which is shown to be the ratio of a transformed boundary layer thickness and the momentum thickness. Since the work involved in correcting these for the effects of pressure gradient was felt to be unwarranted by the smallness of the corrections, the latter were taken to be those established in ref.7. for the steady laminar compressible boundary layer. These corrections are not rigorously justifiable and may be viewed with scepticism. However, because pressure gradients in shock tube channel flows are unlikely to be large and

the corrections themselves are small, it was felt that the ultimate effects of these corrections on the channel flow may be instructive. In fact, the results suggest that pressure gradient corrections to the two parameters mentioned above may be, in general, neglected.

In section II we present the basic integral momentum and mass flow equations for the channel flow as derived by Bernstein . Section III presents the corrections to Bernstein's work for the changing velocity profiles inherent in shock-induced boundary layer flows. In section IV we use the work of the previous two sections to find the ultimate behaviour of the shock tube boundary layer, the inviscid core flow in the channel and the channel running time. The pressure gradient corrections to the form and shape parameters mentioned earlier are discussed in section VI.

II The Channel Flow Integral Momentum and Mass Flow Equations

Referring to Fig. 1, in which the shock tube channel flow is considered relative to the constant strength shock wave, velocity u_w, it may be shown [1] that the integral momentum equation is,

$$\frac{d\bar{\theta}_c}{dx} + \bar{\theta}_c \left\{ (\bar{H}_c + 2) \frac{1}{u_e} \frac{du_e}{dx} + \frac{1}{\rho_e} \frac{d\rho_e}{dx} \right\} = - \frac{\tau_w}{\rho_e u_e^2}, \qquad \text{II.1}$$

where,

$$\left.\begin{aligned} \bar{\theta}_c &= \int_0^{\bar{h}} \frac{\rho u}{\rho_e u_e} \left(\frac{u}{u_e} - 1 \right) \left(1 - \frac{y}{\bar{a}} \right) dy, \\ \bar{\delta}_c^* &= \int_0^{\bar{h}} \left(\frac{\rho u}{\rho_e u_e} - 1 \right) \left(1 - \frac{y}{\bar{a}} \right) dy, \end{aligned}\right\} \qquad \text{II.2}$$

and

$$\bar{H}_c = \frac{\bar{\delta}_c^*}{\bar{\theta}_c}$$

The distances x, y and $\bar{a}$ are respectively the boundary layer development length from the foot of the shock wave, the radial distance from the channel wall and the radius, or hydraulic radius, of the channel. The upper limit of the integrals of equations II.2, $\bar{h}$, is some convenient radial distance from the wall to a point which is always outside the boundary layer; $\bar{h}$ must also be invariant with x. The suffix e refers to quantities evaluated in the inviscid core flow at the distance x from the

origin of the boundary layer and suffix c denotes channel flow parameters. The quantities ρ and τ_w are respectively the density and the wall friction whilst u is the velocity parallel to the X co-ordinate axis and is measured relative to the shock wave.

Note that the form of equation II.1 is the usual form of the pipe flow integral momentum equation but that the direction of the wall friction is reversed. This is due to the fact that, in the co-ordinate system taken relative to the shock wave, the wall moves with the velocity u_w which is always greater than u_e, the inviscid core flow velocity.

The mass flow equation may be written as

$$\frac{\rho_e u_e}{\rho_{eo} u_{eo}} = 1\Big/\left(1 + \frac{2\bar{H}_c \bar{\theta}_c}{a}\right), \qquad \text{II.3.}$$

where suffix eo refers to quantities evaluated directly behind the shock wave.

By the direct differentiation of equation II.3 with respect to X it is possible to obtain an expression for $d\bar{\theta}_c/dx$. Consequently, the elimination of $\bar{\theta}_c$ between equations II.1 and II.3. may be shown to yield,

$$\frac{u_{eo}}{u_e}\frac{d\left(\frac{u_e}{u_{eo}}\right)}{d\left(\frac{x}{a}\right)}\left\{\left(M_e^2-1\right) + \left(\frac{\rho_{eo}u_{eo}}{\rho_e u_e}-1\right)\left(\bar{H}_c + 1 - \frac{\frac{u_e}{u_{eo}}}{\bar{H}_c}\frac{d\bar{H}_c}{d\left(\frac{u_e}{u_{eo}}\right)}\right)\right\}\frac{1}{2\bar{H}_c} = -\frac{\tau_w}{\rho_e u_e^2}. \qquad \text{II 4}$$

Bernstein assumes in ref. 1. that the form of the inviscid core flow may be represented by the one-dimensional isentropic flow equations, in which case the flow quantities in the core flow such as the density, ρ_e, the Mach number, M_e, and the viscosity, μ_e, may be expressed in terms of the core flow velocity, u_e. Hence, in terms of their values aft of the shock wave, these quantities are written as

$$\left.\begin{aligned} \frac{\rho_e}{\rho_{eo}} &= \left[1 + \frac{\gamma-1}{2} M_{eo}^2 \left(1 - \frac{u_e^2}{u_{eo}^2}\right)\right]^{\frac{1}{\gamma-1}}, \\ M_e^2 &= M_{eo}^2 \frac{u_e^2}{u_{eo}^2} \Big/ \left[1 + \frac{\gamma-1}{2} M_{eo}^2 \left(1 - \frac{u_e^2}{u_{eo}^2}\right)\right], \\ \frac{\mu_e}{\mu_{eo}} &= \left(\frac{T_e}{T_{eo}}\right)^{\omega} = \left(\frac{\rho_e}{\rho_{eo}}\right)^{\omega(\gamma-1)} = \left[1 + \frac{\gamma-1}{2} M_{eo}^2 \left(1 - \frac{u_e^2}{u_{eo}^2}\right)\right]^{\omega} \end{aligned}\right\} \quad \text{II S}$$

Consequently, it would appear that, provided relationships can be found for the channel flow boundary layer form parameter, $\bar{H}c$, and the wall friction, τ_w, then we may determine the variation of the inviscid core flow velocity, u_e, with the development length, x.

III. The Form Parameter, $\bar{H}$, and the Wall Friction on a Moving Plate.

Bernstein has shown in ref.1. that the integral momentum equation for the boundary layer induced by the passage of a plane, constant velocity shock wave over a plate has the same form as equation II.1, when the flow is considered relative to the wave. Here again, as in equation II.1, pressure gradient effects are included but we note that the expressions for the momentum and mass flow thicknesses together with the form parameter must be re-defined. They are now, respectively,

$$\left.\begin{aligned} \bar{\theta} &= \int_0^{\bar{h}} \frac{\rho u}{\rho_e u_e}\left(\frac{u}{u_e} - 1\right) dy, \\ \bar{\delta}^* &= \int_0^{\bar{h}} \left(\frac{\rho u}{\rho_e u_e} - 1\right) dy, \\ \text{and} \quad \bar{H} &= \frac{\bar{\delta}^*}{\bar{\theta}} \end{aligned}\right\} \qquad \text{III.1}$$

Here we have dispensed with the suffix e to distinguish between plate flow and channel flow boundary layer parameters.

Bernstein notes that the definitions of the two boundary layer thicknesses, both in equation III.1 and equation II.2, are not the conventional ones in the sense that velocities are not

referred to wall or plate. Conventional definitions of these thicknesses are, therefore,

$$\left.\begin{aligned} \theta &= \int_0^{\bar{h}} \frac{\rho(u_w - u)}{\rho_e(u_w - u_e)}\left(1 - \frac{u_w - u}{u_w - u_e}\right) dy, \\ \delta^* &= \int_0^{\bar{h}} \left\{1 - \frac{\rho(u_w - u)}{\rho_e(u_w - u_e)}\right\} dy, \end{aligned}\right\} \qquad \text{III 2.}$$

and, also, $H = \dfrac{\delta^*}{\theta}$.

By the use of the transformation,

$$Y = \int_0^y \frac{\rho}{\rho_e} dy, \qquad \text{III.3}$$

Bernstein was able to show that,

$$\left.\begin{aligned} \frac{\theta}{\bar{\theta}} &= \frac{1}{\left(\frac{u_w}{u_e} - 1\right)\left(\frac{u_w}{u_e}\left\{H_i - 1\right\} + 1\right)}, \\ \bar{H} &= \frac{\frac{u_w}{u_e} H_i - H}{\left(\frac{u_w}{u_e} - 1\right)\left(\frac{u_w}{u_e}\left\{H_i - 1\right\} + 1\right)}, \end{aligned}\right\} \qquad \text{III.4.}$$

where $H_i = \dfrac{\delta_i^*}{\bar{\theta}_i} = \dfrac{\int_0^{\bar{h}} \left(1 - \frac{u_w - u}{u_w - u_e}\right) dY}{\int_0^{\bar{h}} \frac{u_w - u}{u_w - u_e}\left(1 - \frac{u_w - u}{u_w - u_e}\right) dY}$.

Hence, suffix i is used to denote an 'equivalent' incompressible boundary layer.

In order to derive an expression for H, the form parameter for the flow relative to the plate, Bernstein makes use of the differential form of Crocco's zero pressure gradient plate flow energy equation. Writing this equation in the steady co-ordinate system relative to the shock wave and heeding the boundary condition that at $y=0$, $u = u_w$, he finds on integration that,

$$\frac{\rho_e}{\rho} = \frac{T}{T_e} = \frac{T_w}{T_e} + \left\{ 1 - \frac{T_w}{T_e} + \frac{\gamma-1}{2} M_e^2 \left(\frac{u_w}{u_e} - 1 \right)^2 \right\} \frac{u_w - u}{u_w - u_e} - \frac{\gamma-1}{2} M_e^2 \left(\frac{u_w}{u_e} - 1 \right)^2 \left(\frac{u_w - u}{u_w - u_e} \right)^2, \quad \text{III 5.}$$

where T is the temperature.

Hence, it follows that H is given by

$$H = \frac{T_w}{T_e} H_i + \frac{\gamma-1}{2} M_e^2 \left(\frac{u_w}{u_e} - 1 \right)^2 \qquad \text{III 6}$$

For the purposes of calculation, Bernstein assigns to H_i the Blasius value of 2.59. However, work reported in ref.2, which is based on exact solutions to the problem of the shock-induced boundary layer on a flat plate provided by Mirels (ref.3.), shows that H_i varies with u_w/u_e . Values of H_i against u_w/u_e are shown in Fig. 2. For the purposes of the present calculations we shall take a value of H_i corresponding to a particular value of u_w/u_{eo} , although u_w/u_e increases monotonically with x

in the present problem. The latter variation, however, is due to pressure gradient effects only and is not due to a dependence on the shock strength as considered by Mirels. Furthermore, the variation of H_1 with u_w/u_e is not large between the values of, say, $u_w/u_e = 2$ and $u_w/u_e = \infty$.

In order to obtain an expression for the wall friction τ_w, Bernstein writes the velocity profile relative to the plate in the Pohlhausen quartic approximate form, i.e.,

$$\frac{u_w - u}{u_w - u_e} = \frac{1}{6}\frac{Y}{\Delta}\left(\Lambda + 12\right) - \frac{Y^2}{2\Delta^2}\Lambda - \frac{Y^3}{2\Delta^3}\left(4 - \Lambda\right) + \frac{Y^4}{6\Delta^4}\left(6 - \Lambda\right), \qquad \text{III 7}$$

where Y is given by equation III.3,

$$\Delta = \int_0^\delta \frac{\rho}{\rho_e}\, dy, \qquad \text{III 8}$$

δ being the effective edge of the velocity boundary layer and,

$$\Lambda = \frac{\rho_e \Delta^2}{\left(\frac{u_w}{u_e} - 1\right)} \frac{\mu_w}{\mu_e^2} \frac{d}{dx}\left(u_w - u_e\right). \qquad \text{III 9}$$

Consequently, the expression for τ_w may be written in non-dimensional form as,

$$\frac{\tau_w}{\rho_e u_e^2} = \frac{\frac{\mu_e}{\mu_{e_0}}}{\frac{\rho_e}{\rho_{e_0}}\frac{u_e}{u_{e_0}}} \frac{1}{6}\frac{\Delta}{a} R_{e_0}\left\{\bar{\Lambda} R_{e_0} + 12\left(1 - \frac{u_w}{u_e}\right)\right\}, \qquad \text{III 10a}$$

$$\left.\begin{aligned} &\text{where} \qquad R_{e_0} = \frac{\rho_{e_0} u_{e_0} \bar{a}}{\mu_{e_0}}, \quad * \\ &\text{and} \qquad \bar{\Lambda} = \left(\frac{\Delta}{\bar{a}}\right)^2 \frac{\bar{\mu}_w}{\bar{\mu}_{e_0}} \frac{\rho_e}{\rho_{e_0}} \frac{d\left(\frac{u_e}{u_{e_0}}\right)}{d\left(\frac{x}{\bar{a}}\right)} = -\frac{\Lambda\left(\frac{u_w}{u_e}-1\right)}{R_{e_0}} \end{aligned}\right\} \quad \text{III 10b}$$

Writing

$$\left.\begin{aligned} f &= \frac{\Delta}{\theta}, \\ \text{and } \bar{f} &= \frac{\Delta}{\bar{\theta}} = f\frac{\theta}{\bar{\theta}}, \end{aligned}\right\} \quad \text{III 11}$$

Bernstein shows, using equation III.4, that,

$$\bar{f} = \frac{f}{\left(\frac{u_w}{u_e}-1\right)\left(\frac{u_w}{u_e}\left\{H_c-1\right\}+1\right)}. \quad \text{III 12.}$$

Hence, equation III.10 may be re-written as,

$$\frac{\tau_w}{\rho_e u_e^2} = \frac{\frac{\mu_e}{\mu_{e_0}}}{\frac{\rho_e u_e}{\rho_{e_0} u_{e_0}}} \frac{1}{6R_{e_0}} \frac{\left(\frac{u_w}{u_e}-1\right)\left(\frac{u_w}{u_e}\left\{H_c-1\right\}+1\right)}{f\frac{\bar{\theta}}{\bar{a}}} \left\{\bar{\Lambda} R_{e_0} + 12\left(1-\frac{u_w}{u_e}\right)\right\}. \quad \text{III 13}$$

---

*Note that in the formation of the Reynolds number, Reo, $\bar{a}$ is used as the significant length. For the moment, $\bar{a}$ may be taken to denote any significant length, say the length of the plate. However, its ultimate purpose is to reconcile the expression for τ_w, equation III.10, with equation II.4 at which stage $\bar{a}$ will again be taken to mean the channel radius.

In order to provide values for f in our present calculations we take account of the variation of f with ω , the index in the viscosity-temperature relationship $\mu \propto T^{\omega}$. With the aid of the results presented in ref.4, the approximate expression for f for a flat plate boundary layer may be shown to be,

$$f = [f]_{\omega=1} \left[\beta_1 + (1-\beta_1)\frac{T_w}{T_e} + \beta_2 \sigma^Z \tfrac{\gamma-1}{2} M_e^2 \left(\frac{u_w}{u_e}-1\right)^2 \right]^{1-\omega}, \qquad \text{III 14.}$$

where β_1 is a function of u_w/u_e , β_2 may be taken to be 0.31, σ is the Prandtl number and,

$$\left.\begin{aligned} Z &= 0.42 - 0.095\left(\frac{u_w}{u_e}-1\right)^n, \\ n &= -0.4(\omega-1) + 0.34 \end{aligned}\right\} \qquad \text{III 15}$$

where,

In his calculations presented in ref.1., Bernstein takes $[f]_{\omega=1}$ to be 9.072 (the value obtained by matching the Blasius solution to the Pohlhausen profile, equation III.7, with $u_w/u_e = 0$), whilst β_1 and β_2 are taken to be the values given by Young (ref.5.) for $u_w/u_e = 0$, namely 0.45 and 0.18. The index Z is also chosen in accordance with the work of ref.5, as 0.5. Again, as was the case for H_1, results obtained from Mirels' work in ref.3 (see ref.2) show that the parameter $[f]_{\omega=1}$ varies with u_w/u_e.

A graph of this variation is included in Fig.2. For the same reasons as those outlined earlier in the discussion on the choice of H_1, we shall take in our present calculations values of $[f]_{\omega=1}$ corresponding to the particular values of u_w/u_{e0} chosen. Similarly, the variation of β_1 with u_w/u_e given in ref.4 may be modified in this respect to give,

$$\beta_1 = 0.36 - 0.06 \frac{u_w}{u_{e0}}. \qquad \text{III } 16$$

$\overline{\text{IV}}$ The Boundary Layer Development and Running Time in a Shock Tube Channel.

Bernstein argues in ref.1 that in order to solve the combined momentum and mass flow equation (equation II.4) we may approximate to the two unknowns, $\bar{H}_o$ and τ_w, by the use of the values of the equivalent plate flow parameters presented in section III. Consequently, we may use equations III.4 and III.6 together with the approximation,

$$\bar{H}_o \simeq \bar{H}, \qquad \overline{\text{IV}}.1$$

which is then used with equation II.4. We see from a comparison of equations II.2 and III.1 that the above approximation is most accurate when the values of $y/\bar{a}$ inside the boundary layer are very much less than unity. However, as Bernstein argues, since $\bar{H}_c$ and $\bar{H}$ represent the ratio of two boundary layer thicknesses, the approximation may well be adequate for larger values of $y/\bar{a}$. We may also make use of the equations III.4 and III.6 to obtain an expression for the term $\frac{u_e}{u_{eo}} \frac{d\bar{H}_c}{d\left(\frac{u_e}{u_{eo}}\right)}$ which occurs in equation II.4. Bernstein shows that this relationship is of the form,

$$\frac{\frac{u_e}{u_{eo}} \frac{d\bar{H}_c}{d\left(\frac{u_e}{u_{eo}}\right)}}{\bar{H}_c} = 1 + \overline{\gamma-1} M_e^2 + \frac{\frac{u_w}{u_e}}{\frac{u_w}{u_e}-1}\left[1 - \frac{\bar{H}_i}{\bar{H}_c}\left(1 + \overline{\gamma-1} M_e^2\right)\right] - \frac{\bar{H}_i}{H_i}\left[1 - \frac{\overline{\gamma-1} M_e^2}{\bar{H}_c}\right]. \qquad \overline{\text{IV}}\,2$$

As has been argued for the approximation to $\bar{H}_o$, f(or $\bar{f}$) represents the ratio of the two boundary layer thicknesses and Bernstein therefore uses in equation II.4 the approximation,

$$f_o \simeq f, \qquad \overline{IV}.3$$

which is used in conjunction with equation III.13, the term in $\frac{\bar{\theta}}{\bar{a}}$ being eliminated from the latter by the use of equation II.3

Note that the approximations used above for H and f are strictly valid not only for plate flows but also for flows with zero pressure gradient. In section $\overline{V}$ tentative corrections to H and f for the effects of pressure gradient are suggested.

We denote the conditions ahead of and immediately aft of the shock wave by suffices 1 and 2, writing a_1 for the sound speed in region 1, M_{S1} for the Mach number of the shock wave ($M_{S1} = u_w/a_1$). Assuming that the temperature in region 1 is the same as the wall temperature aft of the shock wave, Bernstein shows that,

$$\left.\begin{aligned} R_{eo} &= M_{S1} R_1 T_{12}^{\omega}, \\ T_{12} &= \frac{T_1}{T_2} \\ \text{where} \quad \text{and} \quad R_1 &= \frac{f_1 a_1 \bar{a}}{\mu_1}. \end{aligned}\right\} \qquad \overline{IV}.4$$

Thus, with the aid of equations $\overline{IV}.1$ - $\overline{IV}.4$, equations III.4, III.6 and III.13, Bernstein shows that equation II.4 reduces to the form,

$$\frac{d\left(\frac{x}{\bar{a}}\right)}{d\left(\frac{u_e}{u_{eo}}\right)} = M_{S1} R_1 T_{12}^{\omega} G\left(\frac{u_e}{u_{eo}}\right), \qquad \overline{IV}.5.$$

where,

$$G\left(\frac{u_e}{u_{eo}}\right) = \frac{\bar{f}_c\left(1-\frac{\rho_e u_e}{\rho_{eo} u_{eo}}\right)}{8\bar{H}_c \frac{\mu_e}{\mu_{eo}} \frac{u_w - u_e}{u_{eo}}}\left[\left(\frac{\rho_{eo} u_{eo}}{\rho_e u_e} - 1\right)\left(\bar{H}_c + 1 + \frac{\bar{f}_c}{6}\frac{\mu_w}{\mu_e} - \frac{\frac{u_e}{u_{eo}}}{\bar{H}_c}\frac{d\bar{H}_c}{d\left(\frac{u_e}{u_{eo}}\right)}\right) + M_e^2 - 1\right]. \qquad \overline{IV}.6.$$

The numerical integration of equation $\overline{IV}.5$ now yields the variation of u_e with x.

In the case of the shock tube, the point x = 0, t = 0 (the time t being measured from the instant of diaphragm burst) represents the 'origin' of the shockwave. At this point, therefore, the shock wave and contact surface coincide (see Fig.3). Now, since the contact surface in the inviscid core flow represents the first particles of gas set in motion by the shock wave, we see that the time taken for the core flow at the contact surface to develop to a velocity u_e at a distance x from the shock wave is,

$$t = \int_0^x \frac{dx}{u_e} \qquad \overline{IV}\ 7$$

With the aid of equations $\overline{IV}.5$ and $\overline{IV}.6$ the time t may be shown to be,

$$t = \frac{\bar{a}}{u_{eo}} M_{s1} R_1 T_{12}^{\omega} \int_1^{\frac{u_e}{u_{eo}}} \frac{G}{\frac{u_e}{u_{eo}}} d\left(\frac{u_e}{u_{eo}}\right) \qquad \overline{IV}.8.$$

Furthermore, considerations of the geometry of Fig.3. show that the

running time, or hot flow duration between shock wave and contact surface, is,

$$t_R = \frac{x}{u_w}, \qquad \text{IV.9.}$$

and that the corresponding distance from the diaphragm at which this running time occurs is,

$$x' = t.u_w - x. \qquad \text{IV.10}$$

Following ref.6, we are thus able to form the following non-dimensional parameters:

$$\left.\begin{aligned} X &= \frac{10^4 x}{R_1 \bar{a}}, & T &= \frac{10^4 t u_{e_0}}{R_1 \bar{a}}, \\ X' &= \frac{10^4 x'}{R_1 \bar{a}}, & T_R &= \frac{10^4 t_R a_1}{R_1 \bar{a}}. \end{aligned}\right\} \qquad \text{IV.11}$$

In ref.6. values of X,T,X', and T_R were calculated using values of H and f provided by Bernstein and which, in section III, are shown to be in error. Consequently, values of X,T,X' and T_R have been re-calculated in the light of the work of section III. The effects of pressure gradient on the values of these non-dimensional parameters are considered in the following section.

$\overline{V}$ Corrections to H and f for the Effects of Pressure Gradient

We recall that in section III expressions were provided for H and f which were derived from considerations of shock-induced boundary layers on flat plates. Since pressure gradient effects are included in all the relevant expressions required for the integration of equations $\overline{IV}.5$ other than those for H and f (equations III.6 and III.14) it would be of interest to examine how the effects of pressure gradient may modify these and, ultimately, the effect upon the variation of u_e with x. Although no rigorous corrections are available for this type of boundary layer when a pressure gradient is introduced along the wall, corrections are available for the case of the steady compressible laminar boundary layer (which corresponds to the case for which $u_w/u_e = 0$). Now, in considering the latter case in their 'first simple method' Luxton and Young in ref.7 show that the form parameter H may be written as,

$$H = \frac{T_w}{T_e} H_i + \frac{\gamma-1}{2} M_e^2, \qquad \overline{V}.1$$

and this expression is shown to be valid for zero or small pressure gradient flows. We may compare equation $\overline{V}.1$ with the corresponding equation III.6 for the shock-induced boundary layer case and we note that the latter equation reduced to the former if $u_w/u_e = 0$ and H_i is chosen appropriately. We note that in equation III.6 (the shock-induced case) and in equation $\overline{V}.1$, $M_e\left(\frac{u_w}{u_e}-1\right)$

and Me respectively both denote the Mach number of the flow external to the boundary layer relative to the wall. Hence, we see that there is a strong similarity in the behaviour of the form parameter if based on velocities which are referred to the wall. This similarity in the behaviour of H may be seen to extend to f since, according to Luxton and Young,

$$f = [f]_{\omega=1} \cdot \left[\beta_1 + (1-\beta_1)\frac{T_w}{T_e} + \beta_2 \sigma^{\frac{1}{2}} \frac{\gamma-1}{2} M_e^2 \right]^{1-\omega}, \qquad \underline{V}.2$$

for the steady flat plate boundary layer. This expression may be compared with equation III.14 for the shock-induced case but in equation $\underline{V}.2$ $\beta_1 = 0.45$, $\beta_2 = 0.18$ and we note a slight discrepancy in the index to the Prandtl number, σ . Also in equation $\underline{V}.2$ $[f]_{\omega=1}$ must be chosen to agree with the condition that $u_w/u_e = 0$.

In order to correct equations $\underline{V}.1$ and $\underline{V}.2$ for the effects of pressure gradient, Luxton and Young in ref.7 suggest in their 'complete method' the corrected quantities H' and f' where,

$$H' = \frac{T_w}{T_e} H_i + \frac{\gamma-1}{2} M_e^2 + k_2 \lambda \frac{T_r}{T_e}, \qquad \underline{V}\,3$$

$$f' = f(1 + k_1 \lambda), \qquad \underline{V}\,4$$

$$\text{where,} \quad \lambda = \frac{du_e}{dx}\Delta^2 \rho_e \frac{\mu_w}{\mu_e^2}, \qquad \text{V.5.}$$

$$\text{and} \quad \frac{T_r}{T_e} = 1 + \frac{\gamma-1}{2} M_e^2 \sigma^{\frac{1}{2}}, \qquad \text{V.6.}$$

Tr being the recovery temperature. The origin of the non-dimensional pressure gradient term, λ, may be found in the representation of the velocity profile as a Pohlhausen quartic in y/Δ (defined in equations III.3 and III.8). Now, in section III it was seen that from a Pohlhausen point-of-view, the relevant non-dimensional pressure gradient parameter for the shock-induced boundary layer was Λ, defined in equation III.9. Consequently, in considering an appropriate correction for the shock-induced boundary layer we shall write,

$$H' = \frac{T_w}{T_e} H_i + \frac{\gamma-1}{2} M_e^2 \left(\frac{u_w}{u_e} - 1\right)^2 + K_2 \Lambda \frac{T_r}{T_e}, \qquad \text{V.7}$$

$$f' = f\left(1 + K_1 \Lambda\right), \qquad \text{V 8}$$

$$\text{where, now,} \quad \frac{T_r}{T_e} = 1 + \frac{\gamma-1}{2} M_e^2 \left(\frac{u_w}{u_e} - 1\right)^2 \sigma^Z. \qquad \text{V 9.}$$

The index Z is given by equation III.15. In the choice of values of K_1 and K_2 we are restricted to the values given by Luxton and Young for the case of $u_w/u_e = 0$. In ref.7, values

of K_1 and K_2 are plotted against the parameter S_w , where,

$$S_w = \frac{T_w}{T_r} - 1, \qquad \underline{V}.10$$

and in determining K_1 and K_2 from this source, we shall take Tr to be given by equation $\underline{V}.9$. Also, it is noted that the values of K_1 and K_2 as given by Luxton and Young depend upon whether or not the pressure gradient is favourable or adverse. The sign of Λ for the shock-induced boundary layer case implies that the pressure gradient is favourable, and indeed, considering the core flow relative to the wall, it will be seen that gas elements will always accelerate. Consequently, values of K_1 and K_2 will be selected from those given for a favourable pressure gradient.

Although the approximations $\underline{V}.7$ and $\underline{V}.8$ are extremely tentative, it is felt that, since the pressure gradients induced in the core flow of a shock tube are unlikely to be large, the approximations may be permitted. However, we note that even if the forms of the corrections incorporated in equations $\underline{V}.7$ and $\underline{V}.8$ are correct, the parameters K_1 and K_2 will probably be functions of, say u_w/u_{eo} .

For the purposes of calculation we shall retain the rule explained in section III that, in the selection of values for

H_1 and $[f]_{\omega=1}$, we shall choose values appropriate to the values of u_w/u_{eo}. We shall calculate values of $\bar{H}$ and $\bar{f}$ using equations III.4 and III.2 as before, equating these quantities to $\bar{H}_o$ and $\bar{f}_o$ as suggested in section $\underline{\underline{IV}}$. However, the expressions for H' and f' (equations $\underline{\underline{V}}.7$ and $\underline{\underline{V}}.8$) will replace those for H and f (equations III.6 and III.14) in equations III.4 and III.12 Furthermore, it is now necessary to develop an extended expression for $\frac{\bar{u}_e}{\bar{u}_{eo}}\frac{d\bar{H}_c}{\bar{H}_c\, d\left(\frac{u_e}{u_{eo}}\right)}$ based on our new relationship for H', equation $\underline{\underline{V}}.7$. This may be shown to be,

$$\frac{\bar{u}_e}{\bar{u}_{eo}}\frac{d\bar{H}_c}{\bar{H}_c\, d\left(\frac{u_e}{u_{eo}}\right)} = 1 + \overline{\gamma-1}\,M_e^2 + \frac{\frac{u_w}{u_e}}{\frac{u_w}{u_e}-1}\left[1 - \frac{\bar{H}_c}{\bar{H}_c}\left(1+\overline{\gamma-1}\,M_e^2\right)\right] - \frac{\bar{H}_c}{\bar{H}_c}\left[1 - \frac{\overline{\gamma-1}\,M_e^2}{\bar{H}_c}\right]$$

$$+ \frac{k_2\Lambda\,\overline{\gamma-1}\,M_e^2\left(1+\sigma^2\left(\frac{u_w}{u_e}-1\right)\right)}{\bar{H}_c\left(\frac{u_w}{u_e}-1\right)\left(\frac{u_w}{u_e}\left\{H_c-1\right\}+1\right)} - \frac{\frac{u_e}{u_{eo}}\left(1+\frac{\gamma-1}{2}\sigma^2 M_e^2\left(\frac{u_w}{u_e}-1\right)^2\right)}{\bar{H}_c\left(\frac{u_w}{u_e}-1\right)\left(\frac{u_w}{u_e}\left\{H_c-1\right\}+1\right)}\,\frac{d}{d\left(\frac{u_e}{u_{eo}}\right)}\left(k_2\Lambda\right). \qquad \underline{\underline{V}}.11.$$

In order to integrate equation $\overline{IV}.5$ using the pressure gradient corrections contained in equations $\overline{V}.7$, $\overline{V}.8$ and in $\overline{V}.11$ it is necessary to develop some iterative procedure to find the correct value of Λ . Comparing equation III.9 for Λ with equation $\overline{IV}.5$ and making use of equation II.3 it follows that Λ must satisfy the condition,

$$\Lambda = - \frac{\frac{\bar{f}_c^2}{4\bar{H}_c^2}\left(\frac{\rho_{eo}u_{eo}}{\rho_e u_e}-1\right)^2 \frac{\mu_w}{\mu_{eo}}\left(\frac{\mu_{eo}}{\mu_e}\right)^2 \frac{\rho_e}{\rho_{eo}}}{\left(\frac{u_w}{u_e}-1\right) G} . \qquad \overline{V}\ 12.$$

Consequently, starting at $u_e/u_{eo}=1$ and $\Lambda = 0$, we may use equation $\overline{V}.12$ as a check and basis for an iterative procedure at each successive interval in the numerical integration of equation $\overline{IV}.5$ Once the correct value of Λ has been found, the time t may be calculated and hence further values of X,T,X' and T_R obtained.

VI Discussion and Conclusions

The numerical integration of equations IV.5 and IV.8, together with the various supplementary equations which describe the behaviour of the boundary layer and the running time, has been carried-out on the University of London Atlas computer. The results of the calculations based on the analysis of sections II to IV are compared with Bernstein's available results. Thus, Fig.4, which shows the variation of u_e/u_{e0} with $\bar{\theta}/\bar{a}$, includes Bernstein's results for a shock Mach number of $M_{s1} = 2$ only. It is seen in this figure that the agreement is very close. A similar agreement may be noted in Fig.5, which shows the variation of $\bar{H}_0$ with u_e/u_{e0}. Values of Λ shown in Fig.6 and provided by the present work (none of Bernstein's results for Λ are available) indicate that pressure gradient effects become increasingly important as the shock Mach number decreases. Thus we see that the analysis presented in sections II to IV may become increasingly approximate as the shock Mach number decreases. As has been noted in ref.6, boundary layer thicknesses generally increase with decreasing shock Mach number. The increase of Λ with decreasing shock Mach number appears to be consistent with this fact. Thus the zero pressure gradient expressions for H and f presented in section III become increasingly susceptible to error with decreasing shock Mach number. Furthermore,

our earlier assumptions that $\bar{H}_c \simeq \bar{H}$, $\bar{f}_c \simeq \bar{f}$ * may be invalid because of the thickness of the boundary layer at low shock Mach numbers.

Fig.7 shows the variation of X with a_e/u_{t_0} and here we see that appreciable differences occur between the present work and Bernstein's analysis. We note that these differences occur only because of our adjustments to Bernstein's values of H_i and f (see section III). Thus the marked change in X due to these adjustments must be due to the accumulation of the less significant individual changes noted earlier for $\bar{H}_c$ and $\bar{\theta}_e/\bar{a}$.

Graphs of T_R against X' are shown in Figs. 8 & 9 in which are included values of running time measured experimentally. We see in Fig.8 that for $\gamma = 7/5$ the present analysis is in better agreement with the experimental values at the higher shock Mach numbers ($M_{s_1} = 5$ and 6, data by Musgrove (ref.8) and Ackroyd, respectively), whilst for the case of $M_{s_1} = 3$ the present analysis appears to underestimate the running time by approximately the same amount by which the running time was overestimated in ref.6. The results for $M_{s_1} = 1.6$, $\gamma = 5/3$, shown in Fig.9 indicate the same tendency as that noted in Fig.8 for low values of shock Mach number. The experimental results shown in Fig.9 were obtained by Duff (ref.9) and are the only consistent set of results available for $\gamma = 5/3$. Their other claim to importance

*However, as Bernstein has noted, these approximations will be more valid than statements concerning the individual terms in $\bar{H}_c$ and $\bar{H}$; for example $\bar{\theta}_e \simeq \bar{\theta}$.

is the low value of the shock Mach number at which they were obtained. The analytical results for Λ , $M_{s_1} = 1.6$, $\gamma = 5/3$, which are not included in Fig.6, indicate that Λ reaches a maximum value of approximately 0.7 near $u_e/u_{e_0} = 0.3$. Again, the conclusions drawn from Figs. 8 and 9 throw doubt on the validity of the assumptions that $\overline{H}_0 \simeq \overline{H}$, $\overline{f}_0 \simeq f$ and the assumed zero pressure gradient nature of H and f shown in section III. However, we may hope that the results of the pressure gradient corrections to H and f presented in section $\underline{V}$ indicate the likely order of magnitude of the errors in the latter assumption. We shall discuss these results presently. Improvements to the analysis to remove the assumption ($\overline{H}_0 \simeq \overline{H}$, $\overline{f}_0 \simeq f$) do not appear to be worthwhile, since any corrections to the analysis that these improvements provide may well be less significant than the effects of shock attenuation which, strictly, should also be included in the analysis. As shown in ref.6, this type of analysis, based on the integral momentum and mass flow equations, appears to be more reliable than any other in predicting the behaviour of the channel boundary layer and the running time. Thus it would be of interest to examine what the effects of shock attenuation would have on this type of analysis. Another phenomenon which may be comparatively significant, and which has not been included in the analysis, is that of the diaphragm opening time. This may be inferred from some of the more

detailed experimental results shown in ref.6. Note that transition to turbulence in the channel boundary layer has been dealt with in some detail in ref.6 and that those experimental points shown in Fig.8 which may be affected by transition lie at the lower values of T_R and X' and, therefore, do not interest us here.

The corrections to H and f for the effects of pressure gradient suggested in section $\underline{V}$ generally produce results which agree closely with the results based on the simpler expressions derived in section III. The pressure gradient-corrected results are not included in Figs.4-6 for this reason, although the results show that Λ decreases progressively from the values shown in Fig.6 as the shock Mach number decreases. In the iterative procedure used to determine the final value of Λ an acceptable disagreement of 1% was specified between the values of Λ taken at the beginning and end of a cycle. Thus the number of iterative cycles required to determine Λ increased with decreasing shock Mach number. Pressure gradient corrections are included in the results for T_R against X' (Figs. 8 & 9). If we accept these corrections as indicating the order of magnitude which pressure gradient corrections to H and f may provide, then we see that these corrections to H and f are not likely to be as significant as the inclusion of shock attenuation and the finite bursting time of the diaphragm in the analysis.

ACKNOWLEDGEMENTS

The author wishes to thank Prof. A. D. Young and Dr. L. Bernstein for their interest in and comments on the present work.

NOTATION

a_j	Sound speed in region j .
$\bar{a}$	radius, or hydraulic radius.
f	boundary layer parameter defined in equation III.11.
f'	boundary layer parameter corrected for the effects of pressure gradient, see equation V.8
G	function defined in equation IV.6
$\bar{h}$	radial distance from wall to a point which is always outside the boundary layer.
H	boundary layer form parameter, defined in equation III.2
H'	boundary layer form parameter corrected for the effects of pressure gradient see equation V.7.
K_1, K_2	pressure gradient correction parameters which are functions of S_w .
M	Mach number
n	index defined in equation III.15.
R	Reynolds number.
S_j	parameter equal to $\frac{T_j}{T_r} - 1$, see equation V.10
t	time.
T	non-dimensional time, see equation IV.11
T_j	temperature in region j.
u	velocity in the x-direction and measured relative to the shock wave.
x'	distance from the diaphragm
X'	non-dimensional distance from the diaphragm, see equation IV.11

x	Co-ordinate parallel to the wall measured from the foot of the shock wave.
X	non-dimensional form of x, see equation IV.11
y	co-ordinate perpendicular to the wall and measured from the wall.
Y	transformed form of y, see equation III.3
z	index defined in equation III.15.
β_1, β_2	parameters defined in equation III.16.
γ	ratio of the specific heats of the gas at constant pressure and constant volume.
δ	value of y which denotes the edge of the velocity boundary layer.
δ^*	mass flow thickness of the boundary layer, see equation III.2
Δ	transformed form of δ, see equation III.8
θ	momentum thickness of the boundary layer, see equation III.2
λ	non-dimensional pressure gradient parameter, see equation V.5.
μ	coefficient of viscosity.
ρ	density.
σ	Prandtl number.
τ	shear stress
ω	index in the empirical viscosity - temperature relationship, $\mu \propto T^{\omega}$
Λ	non-dimensional pressure gradient parameter, see equation III.9

SUBSCRIPTS

1	refers to conditions ahead of the shock wave.
2	refers to conditions immediately aft of the shock wave.
c	refers to channel flow parameters.
e	refers to conditions in the inviscid core flow outside the boundary layer at a distance x from the origin of the boundary layer.
eo	refers to conditions in the inviscid core flow immediately aft of the shock wave.
i	refers to an 'equivalent' incompressible boundary layer.
r	refers to recovery conditions in the boundary layer.
R	refers to running times.
Sj	refers to a shock wave moving into region j.
w	refers to wall conditions.

Note that the superscript $\bar{}$ refers generally to quantities which are measured relative to the shock wave.

REFERENCES

1. L. Bernstein	Notes on some Experimental and Theoretical Results for the Boundary Layer Development aft of a Shock in a shock tube. A.R.C. C.P.625. April, 1961.
2. J. A. D. Ackroyd	On the Laminar Compressible Boundary Layer with Stationary Origin on a Moving Flat Wall. A.R.C.28 233. August, 1966.
3. H. Mirels	Boundary Layer behind Shock or Thin Expansion Wave moving into stationary Fluid. NACA TN.3712 May, 1956.
4. J. A. D. Ackroyd	On the Laminar Compressible Boundary Layer Induced by the Passage of a Plane Shock Wave over a Flat Wall. A.R.C.28 456. October, 1966.
5. A. D. Young	Skin Friction in the Laminar Boundary Layer in Compressible Flow. Aero Quarterly, Vol.1. pp. 137-164, 1949.
6. J. A. D. Ackroyd	A Study on the Running Times in Shock Tubes. A.R.C. C.P.722. July, 1963.
7. R. E. Luxton and A. D. Young	Generalised Methods for the Calculation of the Laminar Compressible Boundary Layer Characteristics with Heat Transfer and Non-Uniform Pressure Distribution. A.R.C. R and M 3233. January, 1960.
8. J. P. Appleton and P. J. Musgrove	An Investigation of the Departure from Ideal Shock Tube Performance; Preliminary Results. A.R.C.24 721. April, 1963.
9. R. E. Duff.	Shock Tube Performance at Low Initial Pressure. Physics of Fluids, Vol.2, pp.207-216, 1959.

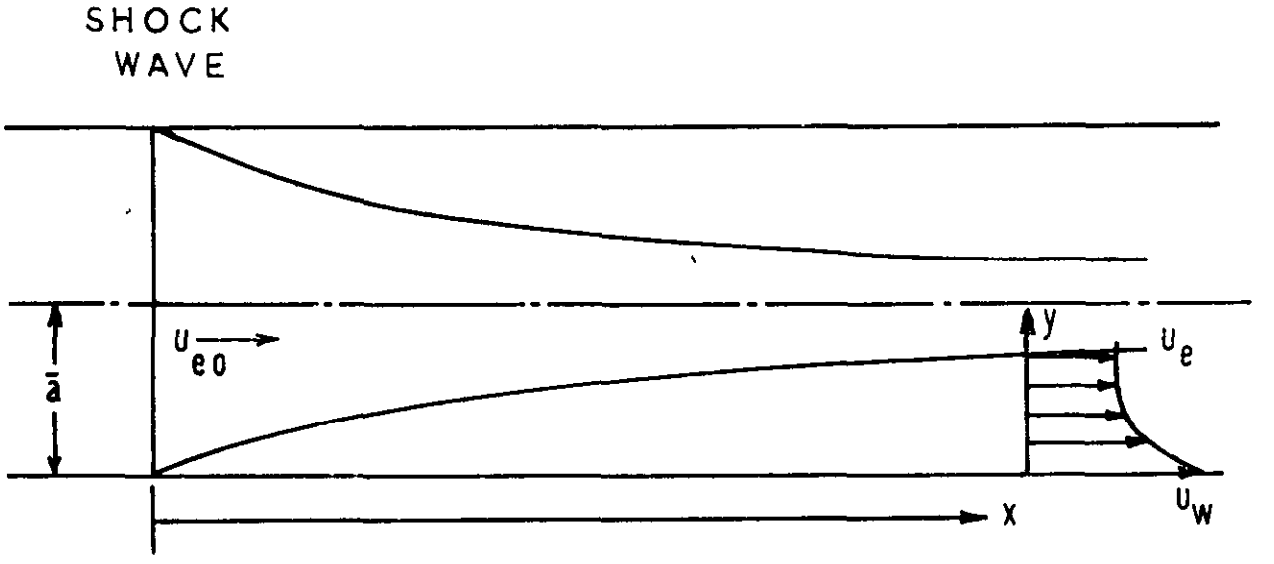

FIG. 1. THE SHOCK TUBE CHANNEL FLOW VIEWED RELATIVE TO THE SHOCK WAVE

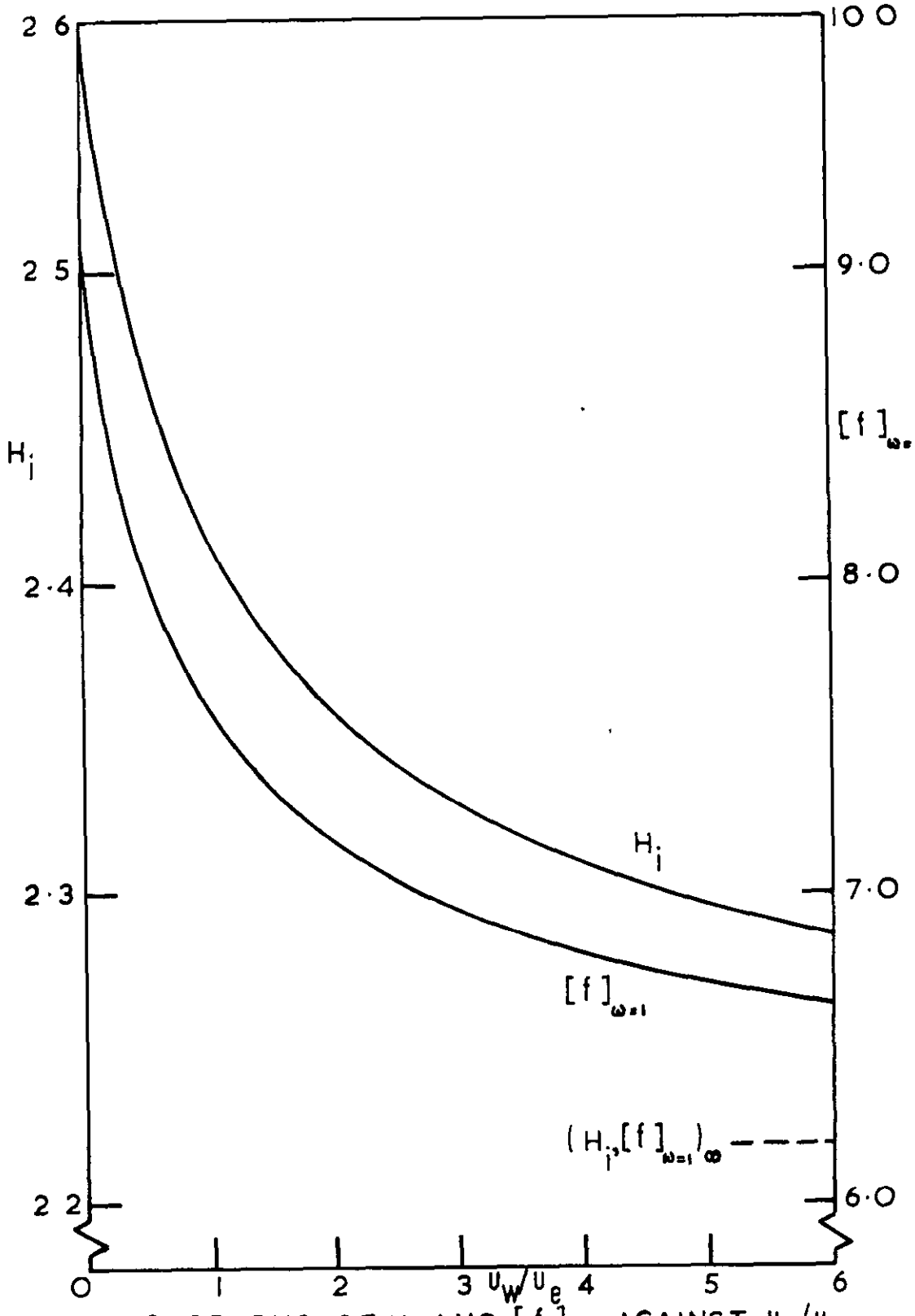

FIG 2 GRAPHS OF H_i AND $[f]_{\omega=1}$ AGAINST u_w/u_e

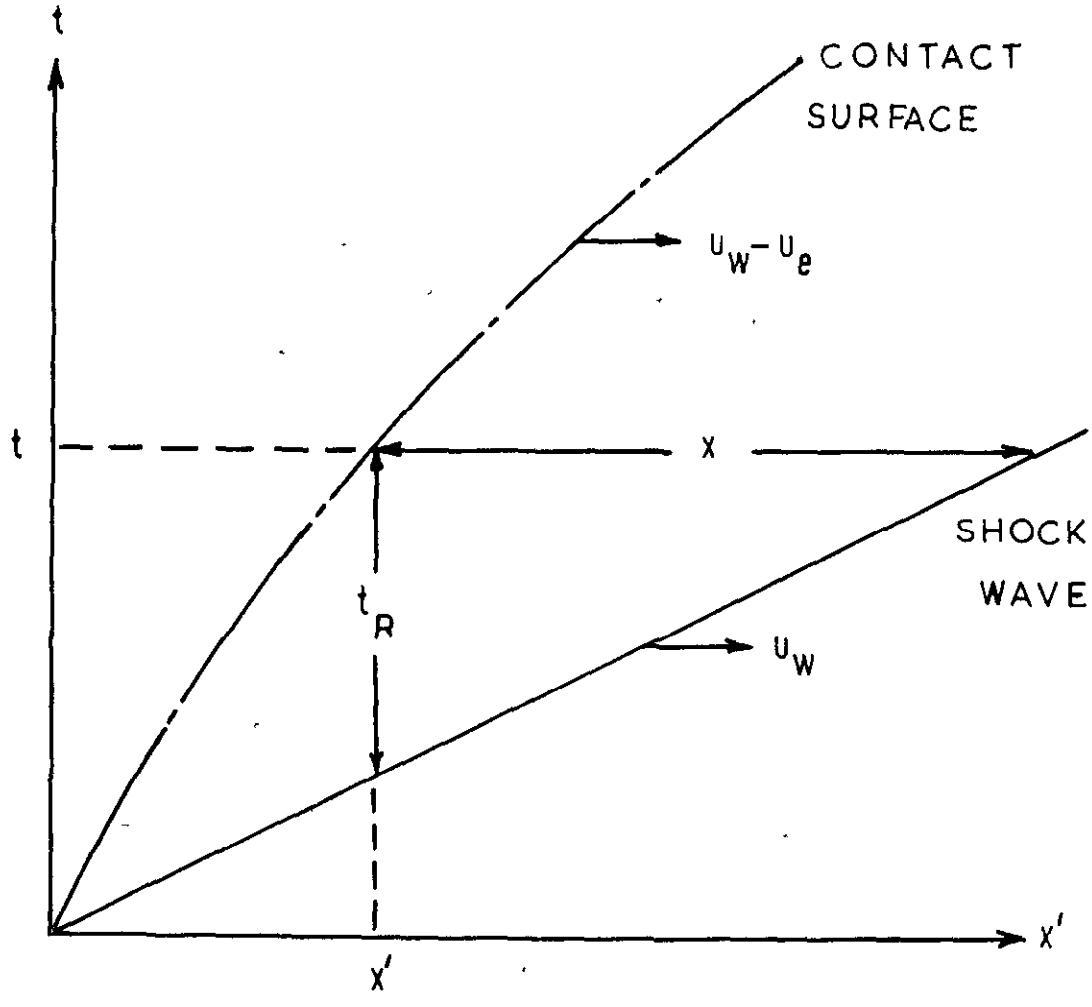

FIG 3 THE x'-t DIAGRAM FOR THE SHOCK TUBE CHANNEL FLOW

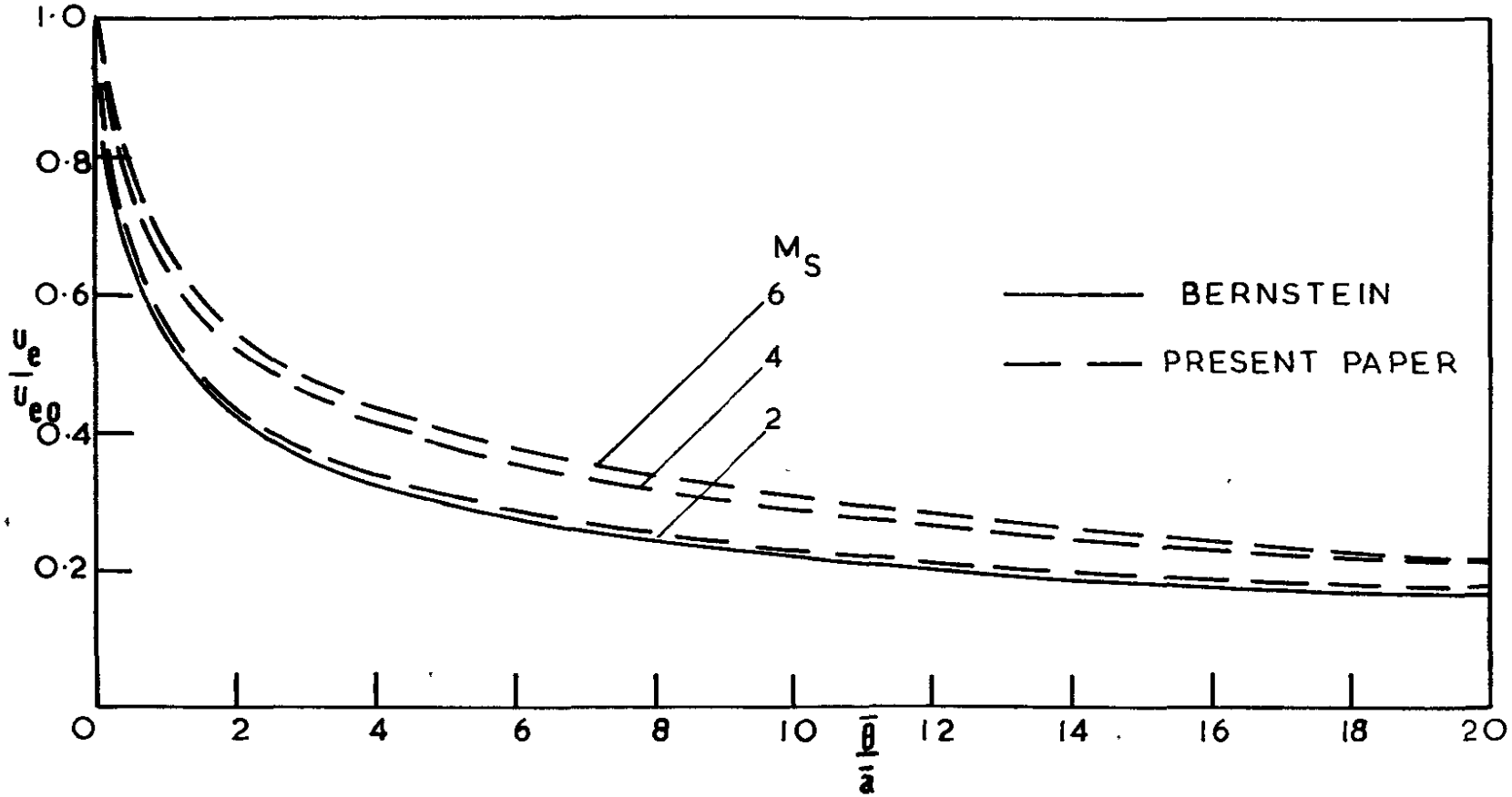

FIG·4 GRAPH OF u_e/u_{e0} AGAINST $\bar{\theta}/\bar{a}$ FOR VARIOUS VALUES OF M_S, $\gamma = 7/5$.

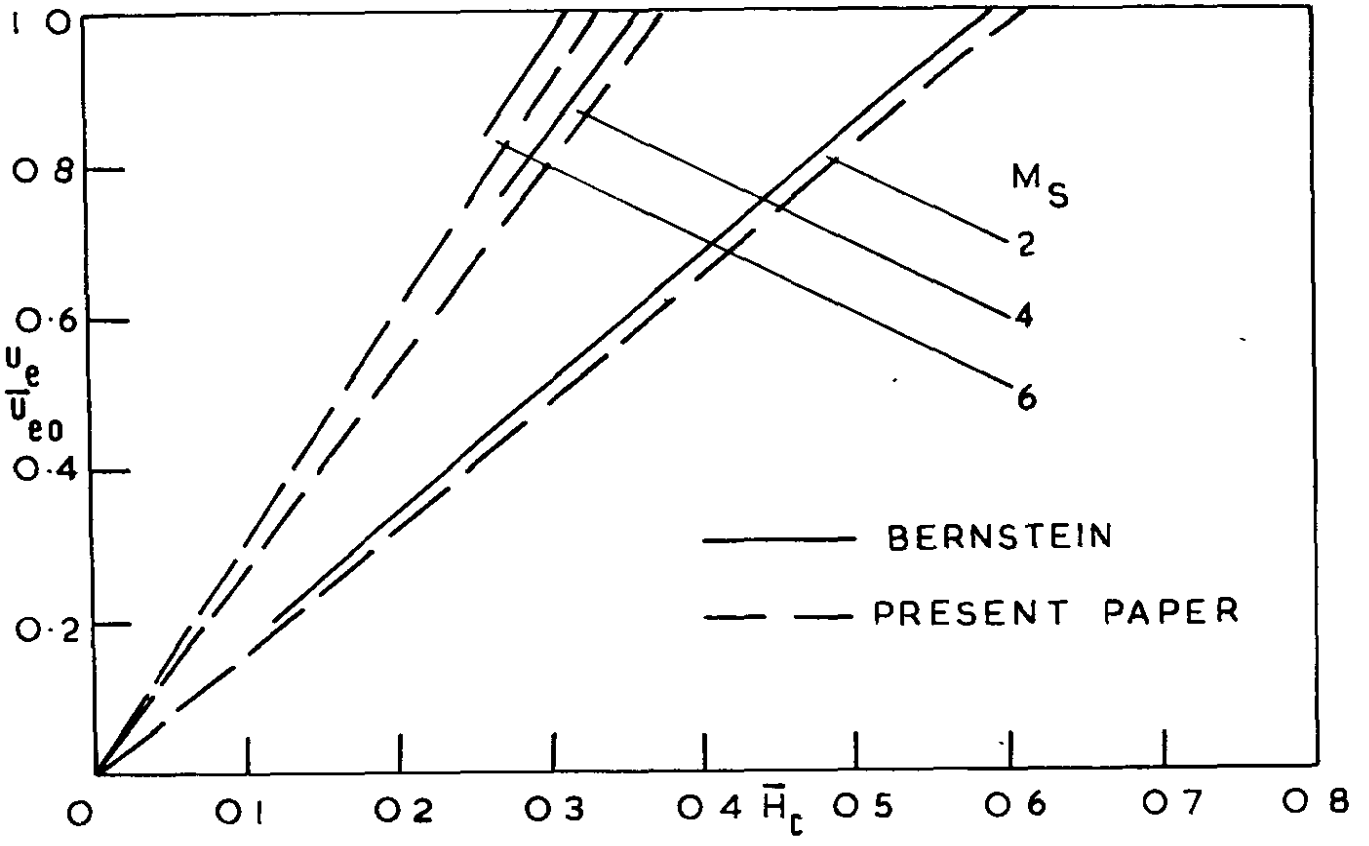

FIG 5 GRAPH OF u_e/u_{e0} AGAINST $\bar{H}_c$ FOR VARIOUS VALUES OF M_S, $\gamma = 7/5$.

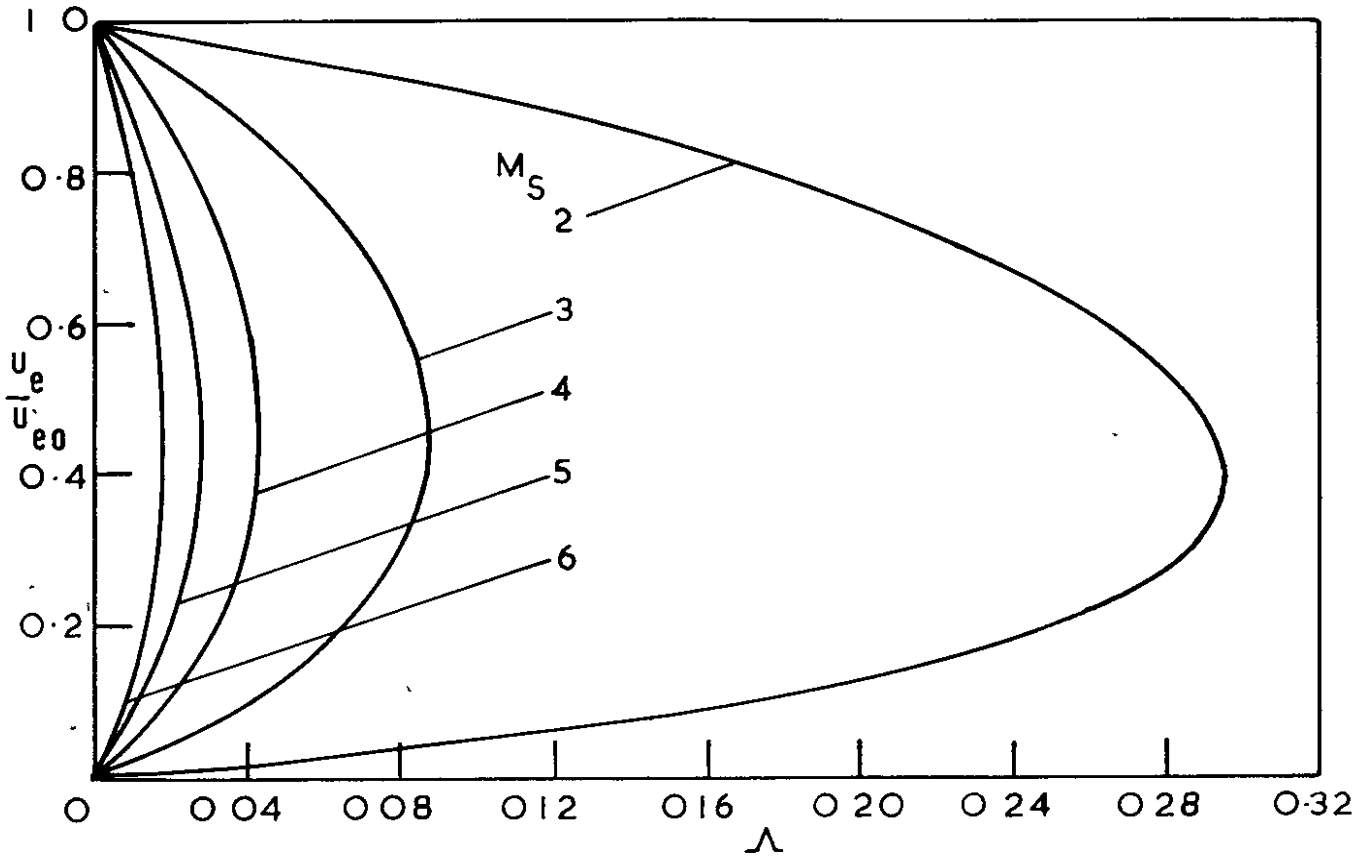

FIG 6 GRAPH OF u_e/u_{e0} AGAINST Λ FOR VARIOUS VALUES OF M_S, $\gamma = 7/5$

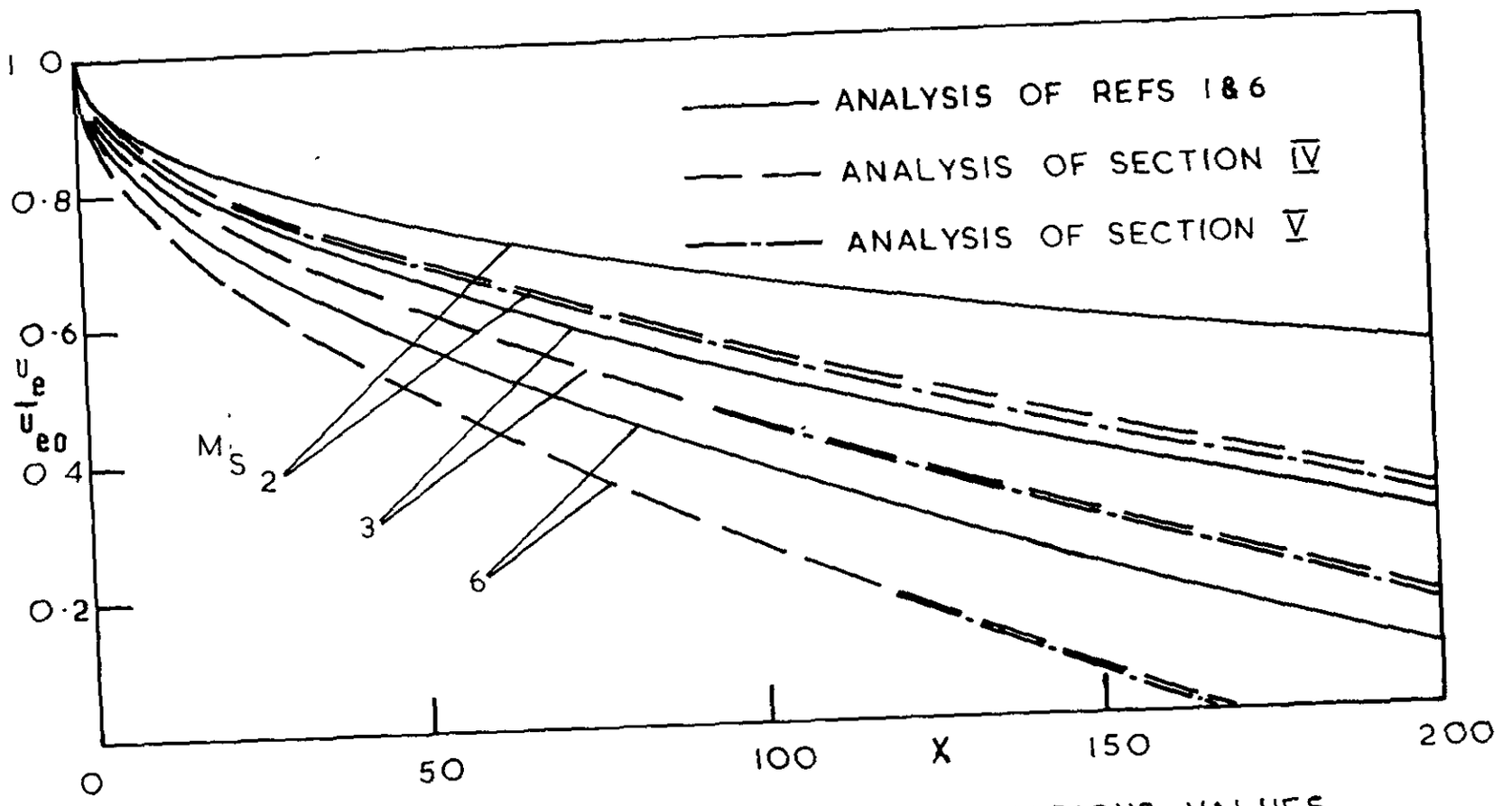

FIG. 7. GRAPHS OF u_e/u_{e0} AGAINST X FOR VARIOUS VALUES OF M_S. $\gamma = 7/5$

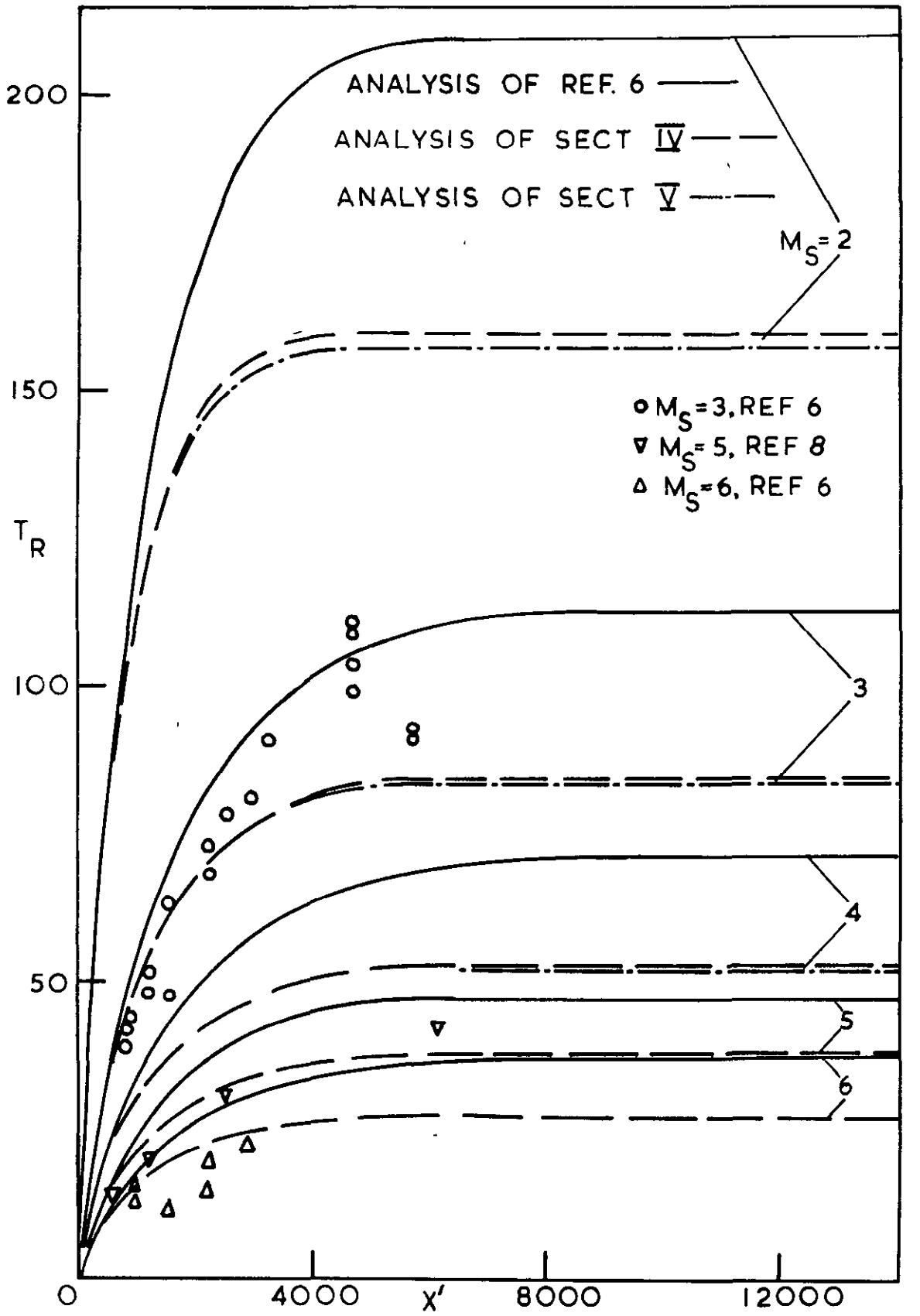

FIG 8 GRAPHS OF T_R AGAINST X' FOR VARIOUS VALUES OF M_S, γ=7/5

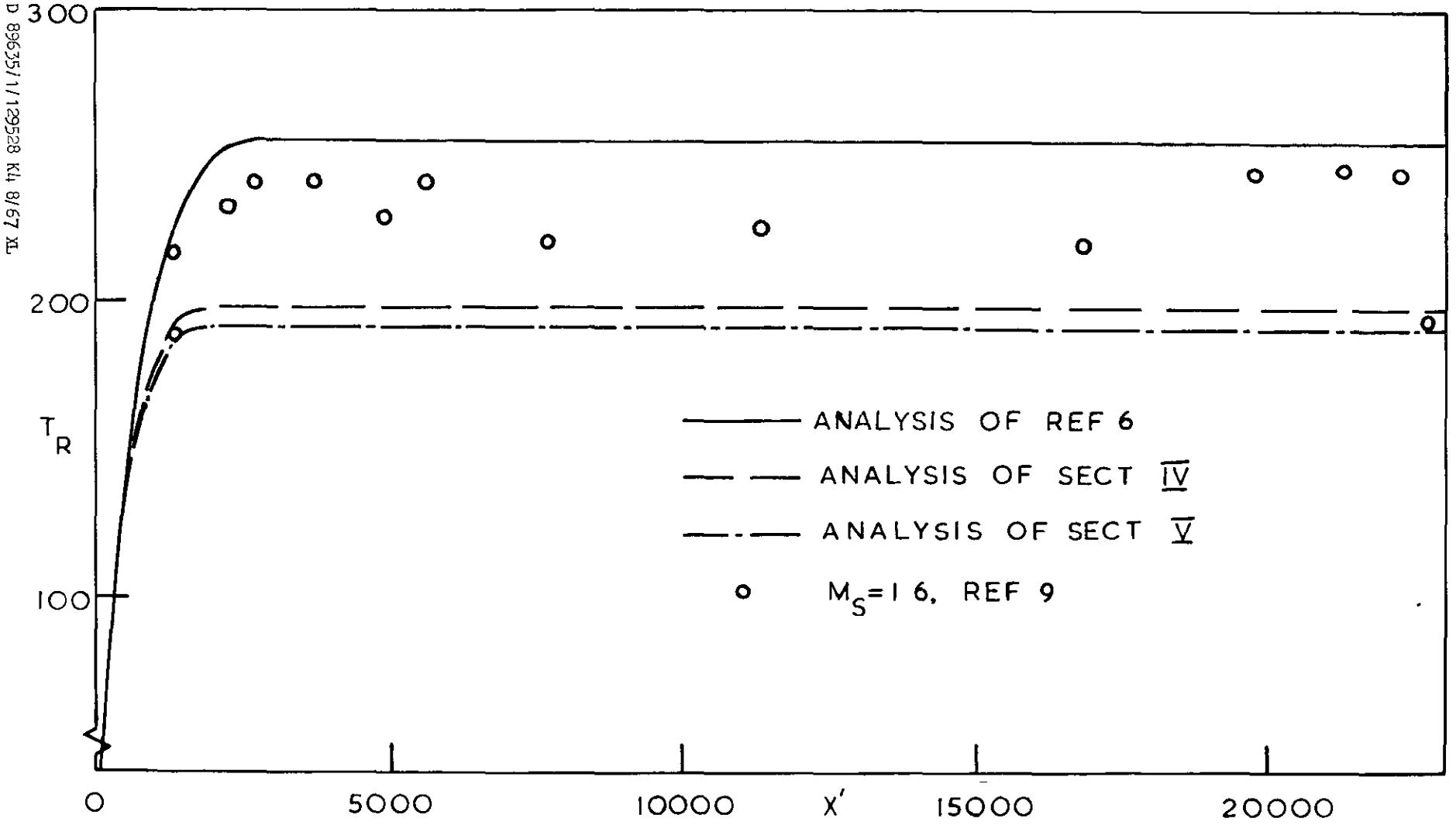

FIG 9 GRAPHS OF T_R AGAINST X' FOR M_S=1 6, γ = 7/5

A.R.C. C.P. No. 966
26.10.66
J. A. D. Ackroyd

SOME FURTHER NOTES ON THE LAMINAR BOUNDARY-LAYER DEVELOPMENT AND RUNNING TIME IN A SHOCK TUBE

Bernstein's analysis of the laminar boundary-layer development aft of a shock wave in a shock tube is corrected in the light of more recent theoretical results. The analysis is extended to include certain pressure gradient corrections. Ackroyd's analysis of the running time in a shock tube, which was based on Bernstein's work, is also re-examined. The corrected results show a significant change in boundary-layer characteristics and running time as compared with Bernstein's results. However, the effects of the additional pressure gradient corrections are shown to be negligible.

A.R.C. C.P. No. 966
26.10.66
J. A. D. Ackroyd

SOME FURTHER NOTES ON THE LAMINAR BOUNDARY-LAYER DEVELOPMENT AND RUNNING TIME IN A SHOCK TUBE

Bernstein's analysis of the laminar boundary-layer development aft of a shock wave in a shock tube is corrected in the light of more recent theoretical results. The analysis is extended to include certain pressure gradient corrections. Ackroyd's analysis of the running time in a shock tube, which was based on Bernstein's work, is also re-examined. The corrected results show a significant change in boundary-layer characteristics and running time as compared with Bernstein's results. However, the effects of the additional pressure gradient corrections are shown to be negligible.

A.R.C. C.P. No. 966
26.10.66
J. A. D. Ackroyd

SOME FURTHER NOTES ON THE LAMINAR BOUNDARY-LAYER DEVELOPMENT AND RUNNING TIME IN A SHOCK TUBE

Bernstein's analysis of the laminar boundary-layer development aft of a shock wave in a shock tube is corrected in the light of more recent theoretical results. The analysis is extended to include certain pressure gradient corrections. Ackroyd's analysis of the running time in a shock tube, which was based on Bernstein's work, is also re-examined. The corrected results show a significant change in boundary-layer characteristics and running time as compared with Bernstein's results. However, the effects of the additional pressure gradient corrections are shown to be negligible.

Printed and published by
HER MAJESTY'S STATIONERY OFFICE

To be purchased from
49 High Holborn, London W C 1
423 Oxford Street, London W 1
13A Castle Street, Edinburgh 2
109 St Mary Street, Cardiff
Brazennose Street, Manchester 2
50 Fairfax Street, Bristol 1
35 Smallbrook, Ringway, Birmingham 5
7 - 11 Linenhall Street, Belfast 2
or through any bookseller

Printed in England

C.P. No. 966

S O Code No 23-9017-